Chinese Chemical Letters 37 (2026) 112189

Contents lists available at ScienceDirect

Chinese Chemical Letters

journal homepage: www.elsevier.com/locate/cclet

Dinuclear Ni enabled reductive diarylation of dienes: Intramolecular comproportionation as the key mechanistic driver

Xiaolong Qi[a,1], Xueli Lv[b,1], Lin Gao[a], Jiwen Jiao[a], Minyan Wang[b,*], Xiaoming Wang[a,c,d,e,*]

[a] State Key Laboratory of Organometallic Chemistry and Shanghai Hongkong Joint Laboratory in Chemical Synthesis, Shanghai Institute of Organic Chemistry, University of Chinese Academy of Sciences, Chinese Academy of Sciences, Shanghai 200032, China
[b] State Key Laboratory of Coordination Chemistry, School of Chemistry and Chemical Engineering, Nanjing University, Nanjing 210093, China
[c] School of Chemistry and Materials Science, Hangzhou Institute for Advanced Study, University of Chinese Academy of Sciences, Hangzhou 310024, China
[d] School of Chemistry and Chemical Engineering, Henan Normal University, Xinxiang 453007, China
[e] Ningbo Zhongke Creation Center of New Materials, Ningbo 315899, China

ARTICLE INFO

Article history:
Received 6 September 2025
Revised 12 November 2025
Accepted 26 November 2025
Available online 29 November 2025

Keywords:
Comproportionation
Difunctionalization
Dinuclear nickel
Reductive coupling
Tetradentate nitrogen ligand

ABSTRACT

The variable oxidation states of nickel catalysts play an essential yet elusive role in reductive coupling reactions, wherein the rapid conversion of nickel species with different oxidation states into Ni^{I} has been recognized as a crucial factor in controlling the catalytic turnover and inhibiting side reactions. Beyond the popular strategies for reductive (re)generation of Ni^{I} species, spontaneous comproportionation of Ni^{0} and Ni^{II} species can form Ni^{I} during catalysis, which is an approach holding great promises yet still relatively underexplored in catalysis. Herein, we transform the intermolecular comproportionation into an entropically more favorable intramolecular pathway by taking advantage of a tetradentate nitrogen ligand (dppn), which effectively brings two catalytic Ni centers in close proximity. This strategy enables ready generation of catalytically active Ni^{I} species for reductive diarylation of dienes with aryl iodides using Mn as the terminal reductant. Mechanistic studies reveal that the dppn ligand facilitates the assembly of a dinickel complex, where one nickel acts as the catalytic site for oxidative addition and coupling while the other nickel functions as an electron reservoir. The intramolecular comproportionation pathway establishes a robust strategy for accessing the often fleeting and elusive Ni^{I} intermediates critical in forging C–C bonds in the reductive coupling reactions.

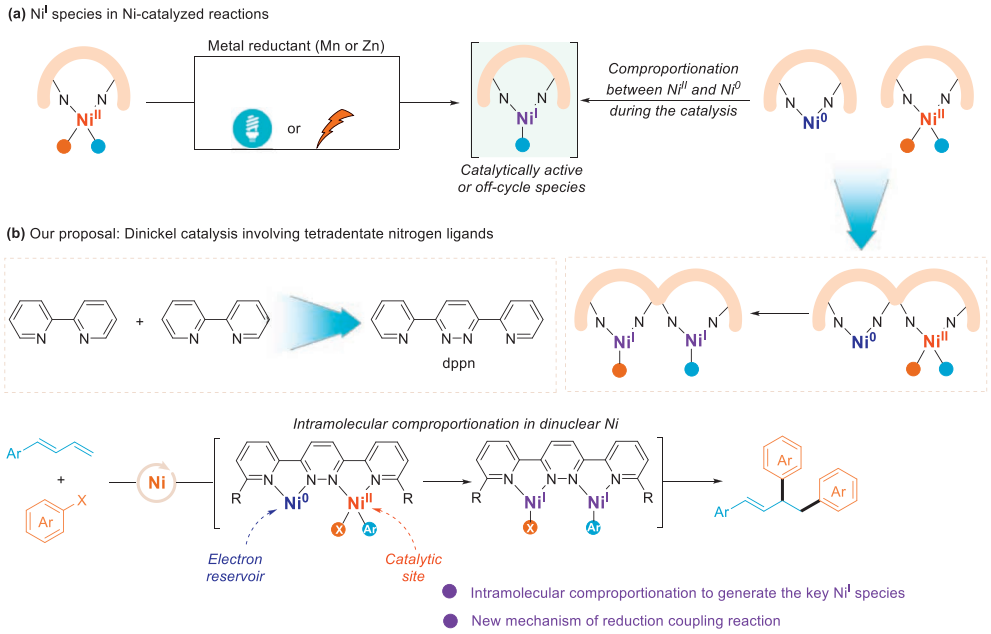
© 2026 Published by Elsevier B.V. on behalf of Chinese Chemical Society and Institute of Materia Medica, Chinese Academy of Medical Sciences.

Inspired from multinuclear metal assemblies in the active sites of metalloenzymes [1,2], bi- (multi-) nuclear metallic catalysis with the potential cooperativity between metal sites within multimetallic catalysts has attracted great attention [3–13]. A prominent example is catalysis by mononuclear nickel complexes, which is featured by unique mechanistic manifolds *via* facile catalyst speciation among Ni^{0}, Ni^{I}, Ni^{II}, and Ni^{III} oxidation states. Notably, recent studies have revealed the involvement of *in-situ* generated dinuclear Ni species or di-Ni-mediated catalytic processes in several catalytic transformations [14–25]. In this context, Uyeda [26,27], Schoenebeck [28–30], our group [31,32] and others have independently demonstrated that dinuclear Ni catalysts, supported by various sophisticated ligands, can exhibit reactivity differing fundamentally from their mononuclear counterparts. These findings highlight the underestimated potential of dinuclear Ni architectures in developing new catalytic paradigms.

Fine-control of the valence states of the catalytic nickel species is crucial for directing reaction pathways and avoiding side reactions. For instance, various reduction strategies have been developed to promote the formation of Ni^{I} species [33–42]. Notably, it has been recognized that in some Ni-catalyzed reactions the comproportionation between Ni^{0} and Ni^{II} intermediates can generate Ni^{I} species, which might be catalytic or off-cycle depending on the reactions studied (Scheme 1a) [43–55]. Inspired by such a spontaneous comproportionation pathway, we envisioned that integrating two bidentate ligand motifs into a single tetradentate framework might enable dual coordination of two metal nuclei in close proximity, which in turn can facilitate an intramolecular comproportionation process that can be favorable for reactions involving Ni^{I} as the catalytic species. Since bipyridine-ligated mononuclear nickel complexes have been established as a class of privileged catalysts in a diverse set of Ni-catalyzed transformations [56–63], we envisaged that the tetradentate dppn ligand

* Correspondence authors.
E-mail addresses: wangmy@nju.edu.cn (M. Wang), xiaoming@sioc.ac.cn (X. Wang).
[1] These authors contributed equally to this work.

https://doi.org/10.1016/j.cclet.2025.112189
1001-8417/© 2026 Published by Elsevier B.V. on behalf of Chinese Chemical Society and Institute of Materia Medica, Chinese Academy of Medical Sciences.



Scheme 1. Transition-metal-catalyzed arylations of 1,3-dienes.

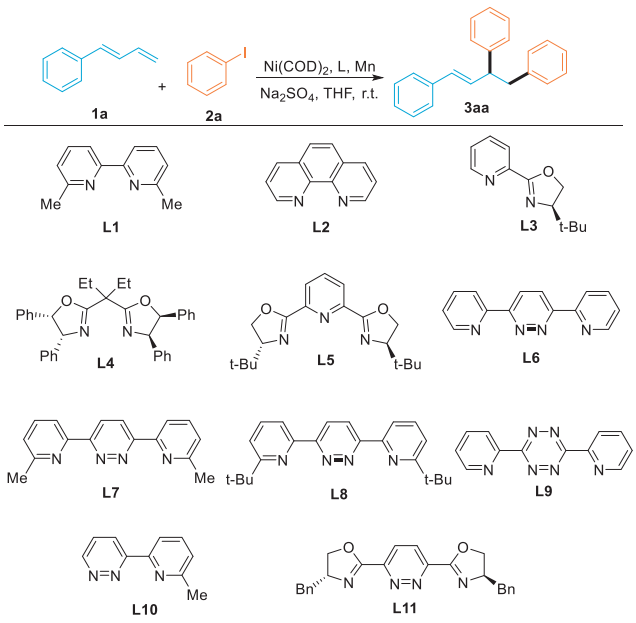
(dipyrido[3,2-a:2′,3′-*c*]phenazine), with two bipyridine units fused *via* a pyridazine linker in its structure, might constitute a promising candidate for our purpose. First synthesized in 1961 [64], dppn has been known to generate mono-, di-, or even polynuclear complexes with diverse metals (Ir, Ru, Rh, Pd, Ni, Cu, *etc.*) [65–71].

Recent development of Ni-catalyzed reductive dicarbofunctionalization of alkenes enables the formation of two new C–C bonds using abundant organic halides [72–88]. Mechanistically [57,74,89–94], one of the most commonly proposed catalytic cycles hinges on the Ni^{I} species as a pivotal intermediate [15,95–102], as demonstrated in the pioneering work by Diao's group [103,104]. Typically, oxidative addition of an electrophile to low-valent Ni^{0} can generate high-valent Ni^{II} intermediate, which can be reduced to Ni^{I} by a reductant prior to olefin insertion. In such events, the reduction of high-valent Ni^{II} intermediates to Ni^{I} governs both catalytic turnover and reaction efficiency, which is generally achieved by exploiting a metal reductant (Zn or Mn) [33], photoredox [34–39] or an electrochemical process [39–44]. Recent advances in reductive diarylation of terminal dienes indeed highlighted the necessity of extra reduction strategies in controlling Ni redox states. Chen's Ni/Cr dual catalysis utilized Cr^{II} as a reductive medium to generate Ni^{I} and aryl radicals for 1,2-diarylation of dienes [105], whereas Wang's electrochemical Ni catalysis achieved real-time reduction of Ni^{II} or Ni^{III} intermediates to sustain Ni^{I} species [106]. Notably, Chen's later work revealed that Ni^{II} intermediates underwent β-H elimination, favoring Heck products over diarylation, even in the presence of the classic Mn reductant [107]. These cases collectively demonstrated that Ni-catalyzed reductive diarylation of dienes relies critically on the reducing Ni^{II} to Ni^{I}, typically via external reductive methods, to enable olefin insertion and suppress undesired β-H elimination pathways.

To continue our studies on the development of dinuclear metallic catalysis [31,32,108–112], we disclose herein a binuclear nickel-catalyzed reductive diarylation of 1,3-dienes using a dppn-type tetradentate ligand, exhibiting exceptional generality for both aryl halides and dienes using Mn as the terminal reductant (Scheme 1b). Mechanistic investigations reveal that the dppn ligand facilitates the assembly of a dinuclear Ni complex, and in the catalytic cycle one Ni center acts as the catalytic site for both oxidative addition and C–C coupling, while the second Ni atom serves as an electron reservoir to turn the oxidation states by intramolecular comproportionation. Crucially, this synergy for the redox event between adjacent Ni centers (Ni^{0}/Ni^{II}) achieves the generation of the key Ni^{I} intermediate timely, which controls the reaction pathways to diarylation of dienes. The results from this work reveals that the use of polydentate nitrogen ligands to develop dinuclear nickel catalysts could open new avenues for advancing nickel-based catalysis.

Firstly, we conducted a screening of the conditions for the template reaction between 1,3-diene **1a** and aryl iodide **2a**, with some commonly used bidentate and tridentate polypyridines as the ligands, and the results were summarized in Table 1. The reactions were typically carried out in THF at room temperature for 12 h, using 10 mol% of $Ni(COD)_2$ and 10 mol% of the specified ligand as the catalyst and 3.0 equiv. of Mn powder as the external reductant, with the yields of the desired diarylation product **3aa** being evaluated by GC determination. Under these conditions, the reaction using bipyridine ligand **L1** afforded only 17 % yield of the desired product **3aa**, and the use of phenanthroline ligand **L2**, Phox ligand **L3**, or Box ligand **L4** even delivered poorer results (<8 % yield). The reaction using the tridentate Pybox ligand **L5** afforded a slightly enhanced yield of **3aa** (21 %). Further survey was conducted on a series of tetradentate ligands, all featured by the presence of a pyridazine ring moiety in the ligand skeleton. To our delight, the yield of **3aa** for the reaction using ligand dppn **L6** boomed up to 75 % under otherwise identical conditions, whereas the reaction using **L7** ligand, with ortho methyl substitution on the pyridine of dppn, furnished an excellent GC yield of 93 % and isolated yield of 85 % for **3aa**. However, using ligand **L8** with a bulk *ortho*-*t*-Bu group, the reaction gave very poor yield (3 %), probably due to the large steric hinderance. Due to the similarity in structure between the tetrazine ligand **L9** and the dppn ligand, we also investigated ligand **L9**. However, the target product **3aa** cannot be obtained. The tetradentate nitrogen ligands dppn **L6** and **L7** exhibited excellent reaction performance in this reaction, which may be due to the coordination of two nickel metals with the four coordination sites of the ligand. The reason for the poor reactivity of ligand **L9** may be that several possible complexes can be formed, and the dinuclear nickel complexes located on opposite sides are more likely to be generated, thus failing to catalyze the reaction. Further,

Table 1
Optimization of diarylation of 1,3-dienes **1a**.[a]



Entry	Cat.	Ligand	Solvent	**3aa** (%)[b]
1	$Ni(COD)_2$	**L1**	THF	17
2	$Ni(COD)_2$	**L2**	THF	5
3	$Ni(COD)_2$	**L3**	THF	5
4	$Ni(COD)_2$	**L4**	THF	8
5	$Ni(COD)_2$	**L5**	THF	21
6	$Ni(COD)_2$	**L6**	THF	75
7	$Ni(COD)_2$	**L7**	THF	93
8	$Ni(COD)_2$	**L8**	THF	3
9	$Ni(COD)_2$	**L9**	THF	2
10	$Ni(COD)_2$	**L10**	THF	57
11	$Ni(COD)_2$	**L11**	THF	1
12	$Ni(COD)_2$	/	THF	5

[a] Reaction conditions: The mixture of **1a** (0.1 mmol), **2a** (0.2 mmol), Mn powder (3.0 equiv.), $Ni(COD)_2$ (10 mol%), Na_2SO_4 (2.1 equiv.) and **L** (**L1**-**L5**, **L10**, 10 mol%) or (**L6**-**L9**, **L11**, 5 mol%) was stirred at room temperature for 12 h.
[b] GC yield.

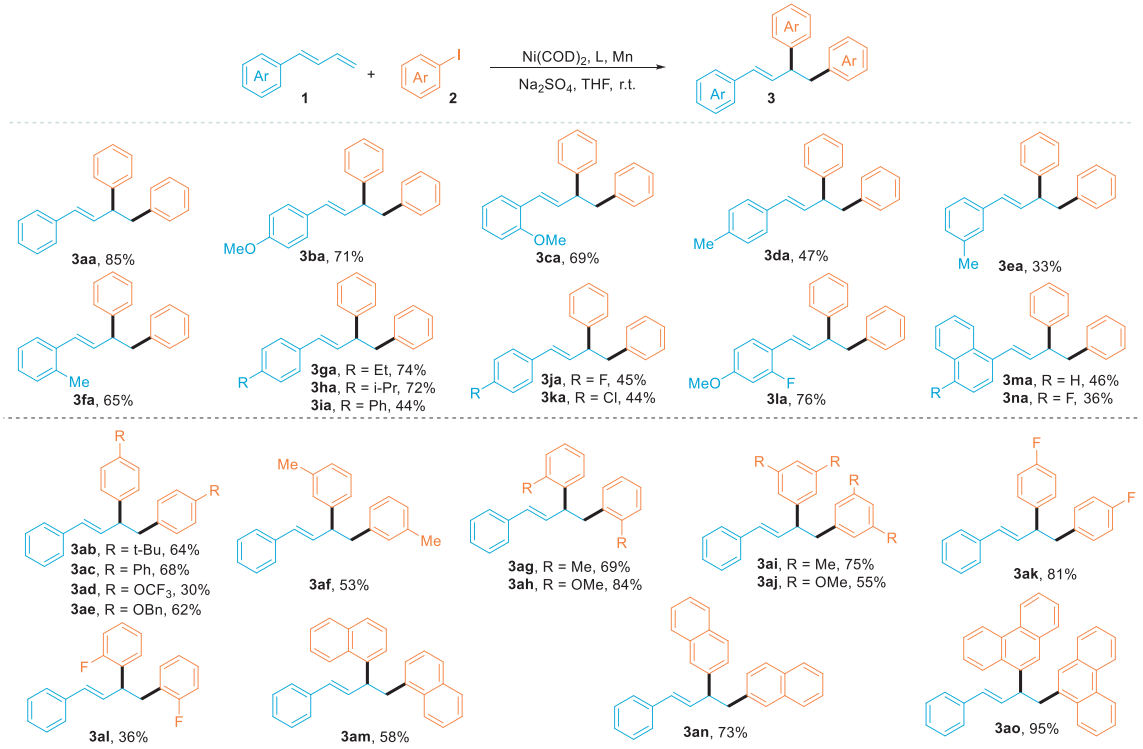
a ligand **L10** was synthesized, by removing a methyl substituted pyridine structure from **L7**. In this case, 57 % yield of **3aa** was obtained along with 1,4-diarylated isomer in a ratio of 5:2 as contrast with the excellent regioselectivity observed using **L7**, hence highlighting the importance of the second pyridyl ring in **L7** for the selectivity control. Although the pyridazine core in **L10** may form a bimetallic Ni catalyst, the instability of the binuclear core likely compromised both activity and selectivity. We have also examined the reaction using ligand **L11**, wherein two pyridine units of dppn have been replaced by two chiral oxazolines. Unfortunately, only trace amount of the desired product was detected in this case. Finally, no **3aa** was detected in the absence of a ligand. Following the successful identification of **L7** as the optimal ligand, additional reaction parameters were also screened in the reaction. While using Zn powder as a reducing agent in the reaction resulted in a decrease in the yield (59 % *vs.* 93 %), using $NiCl_2$·DME as the catalyst precursor afforded a slightly lower yield (83 % *vs.* 93 %).

With the optimized conditions in hand, we proceeded to explore the substrate scope with respect to both dienes and aryl halides. As shown in Scheme 2, a wide range of 1,3-butadienes (**1a-n**) with different steric and electronic natures reacted smoothly with iodobenzene **2a**, affording almost exclusively the 3,4-diarylated *E*-alkene products **3a-n** (regioisomeric ratio > 99:1, *E*/*Z* > 99:1) in moderate to high yields (33 %–85 %), with good functional group compatibility of this protocol. Both electron-donating (methoxy **1b** and **1c**, methyl **1d–1f**, ethyl **1g**, isopropyl **1h**, and phenyl **1i**) and electron-withdrawing (fluoro **1j**, chloro **1k**) groups were all tolerated well in the reactions with **2a**, to generate the corresponding products **3ba–3ka** in 33 %–74 % yields. 1,3-Diene substrate **1l** where multiple positions on the benzene ring (OMe, F) are substituted was also investigated and the reaction also worked smoothly in the reaction, giving the desired product **3la** in 76 % yield. Moreover, the reaction of 1,3-butadiene bearing a naphthyl substituent (**1m**) proceeded smoothly, yielding the corresponding diarylated product **3ma** in 46 % yield. In addition, 1,3-butadiene with a fluoronaphthyl substituent (**1n**) also exhibited good reactivity, providing the corresponding diarylation product **3na** in 36 % yield.

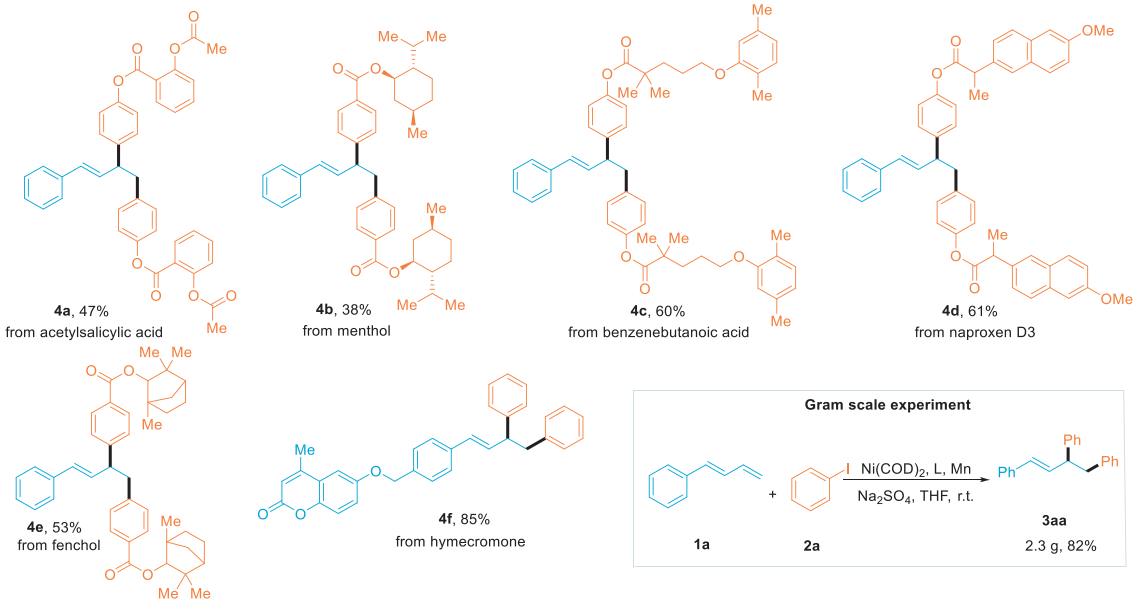
Subsequent substrate scope studies were performed on a variety of substituted aryl iodides using diene **1a** as the coupling partner. Aryl iodides with electron-donating substituents, such as *para*-substituted *tert*–butyl (**3ab**, 64 %), phenyl (**3ac,** 68 %), OCF_3 (**3ad**, 30 %), OBn (**3ae**, 62 %), were found to be compatible with the reaction, affording the corresponding products in good to high yields (30 %–68 %). For aryl iodides with *meta*-substituted methyl groups, the diarylation product **3af** can also be obtained with a yield of 53 %. Diarylation products can also be obtained with moderate to good yields for aryl iodides with *ortho*-substituted groups (**3ag-3ah**, 69 %–84 %). Aryl iodides containing multiple electron donating groups can also perform well in this diarylation reaction (**3ai-3aj**, 55 %–75 %). Diarylation products can also be obtained with moderate to excellent yields for reactions of aryl iodides with electron withdrawing groups (**3ak-3al**, 36 %–81 %). Of practical significance is that various synthetically useful functional groups including F (**3ak-3al**, 36 %–81 %) remain intact during the diarylation reaction. Additionally, substrates containing polycyclic aromatic hydrocarbons can also be well compatible with the protocol (**3am-3ao**, 58 %–95 %). We also attempted to use heteroaryl or alkyl 1,3-butadienes, other alkenes (such as styrene derivatives), as well as aryl bromides and heteroaryl iodides. Unfortunately, these substrates were not applicable to this reaction. In addition, functional groups containing acidic protons (such as -OH, -NH_2, -NHBoc) were incompatible with this reaction. The reductive coupling reactions of diene **1a** with two different aryl iodides under the standard conditions afforded a mixture of homo- and cross-coupling products with poor selectivity.

To further showcase the synthetic utility of the protocol, the late-stage diarylation using the aryl iodides derived from some drugs or bioactive molecules was examined in their reactions with **1a** (Scheme 3). A series of aryl iodides derived from acetylsalicylic acid, menthol, benzenebutanoic acid, naproxen D3 and fenchol, respectively, reacted smoothly with **1a** under the standard conditions to afford the corresponding 3,4-diarylation products **4a-e** in 38 %–61 % yields. Moreover, 1,3-dienes derived from hymecromone was also found to be amenable to the procedure, giving the diarylation products **4f** in 85 % yields, respectively, further attesting the synthetic potential of this method. Furthermore, a gram-scale reaction was performed with 1,3-diene **1a** and aryl iodide **2a** under slightly modified conditions, and the product **3aa** was obtained in 82 % isolated yield (2.3 g) in this case.

Unraveling the identity of catalytically active species and their operative mechanisms poses significant challenges, particularly in the current system employing tetradentate nitrogen ligands like **L7**. We firstly investigated the reaction kinetics of the standard reaction under varying metal/ligand ratios by tracking the quantities of product **3aa** at specified time intervals (Scheme 4a). Under standard conditions (10 mol% [Ni], 5 mol% ligand **L7**), the reaction exhibited a pronounced 4-h induction phase, followed by an accelerated product formation phase that achieved substantial conversion within the subsequent 2 h (Schemes 4a, i). The reaction



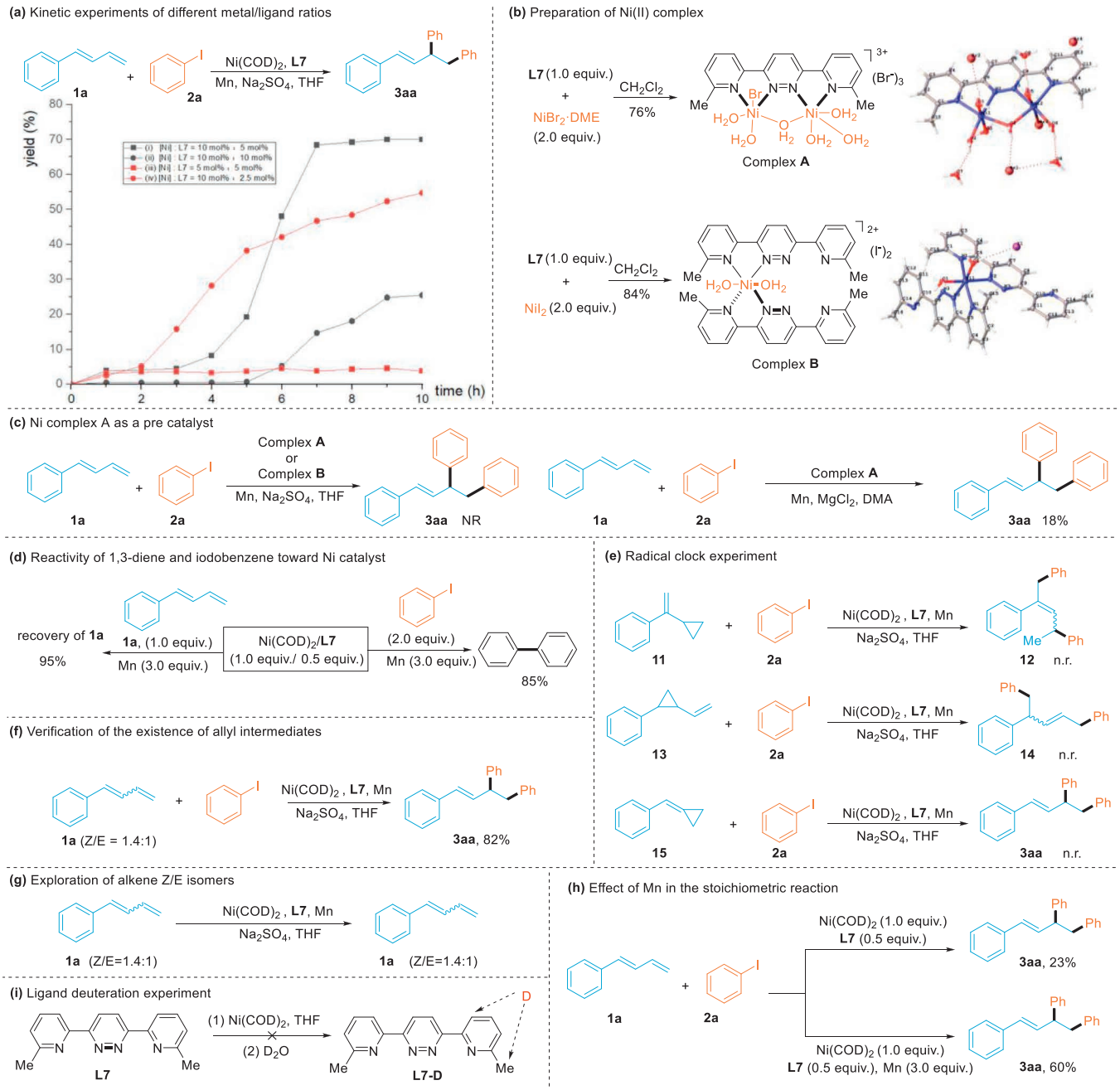
Scheme 2. Substrate scope.



Scheme 3. Late-stage functionalization of drug molecule derivatives.

performance under different ligand to metal molar ratios is much likely an indication of the nature of active species in action, at least to some extent. Therefore, doubling the ligand loading (10 mol% **L7**) while maintaining nickel concentration (10 mol%) was investigated, leading to two critical changes, *i.e.*, the induction period was extended to 5 h and the overall reaction rate diminished significantly (Scheme 4a, ii). More strikingly, when both catalyst components were halfly reduced ([Ni] = **L7** = 5 mol%), the system displayed severely reduced catalytic efficiency, with little product formation even after prolonged 10-h reaction (Scheme 4a, iii). Notably, halving the ligand loading (2.5 mol% **L7**) while keeping 10 mol% [Ni] resulted in a sharply reduced induction time (Scheme 4a, iv, 2 h *vs.* original 4 h) and a higher yield than those employing ligand-excessive conditions (10 mol% [Ni], 10 mol% **L7**). The improved performance under nickel-rich conditions strongly indicates that metal availability critically governs the thermodynamic driving force for dinuclear (or multi-nuclear) intermediate assembly, which might be the catalytically active species.

In the aforementioned kinetic studies, it was found that combining **L7** with 2.0 equiv. of $NiBr_2$·DME in CH_2Cl_2 produced a green



Scheme 4. Mechanistic studies.

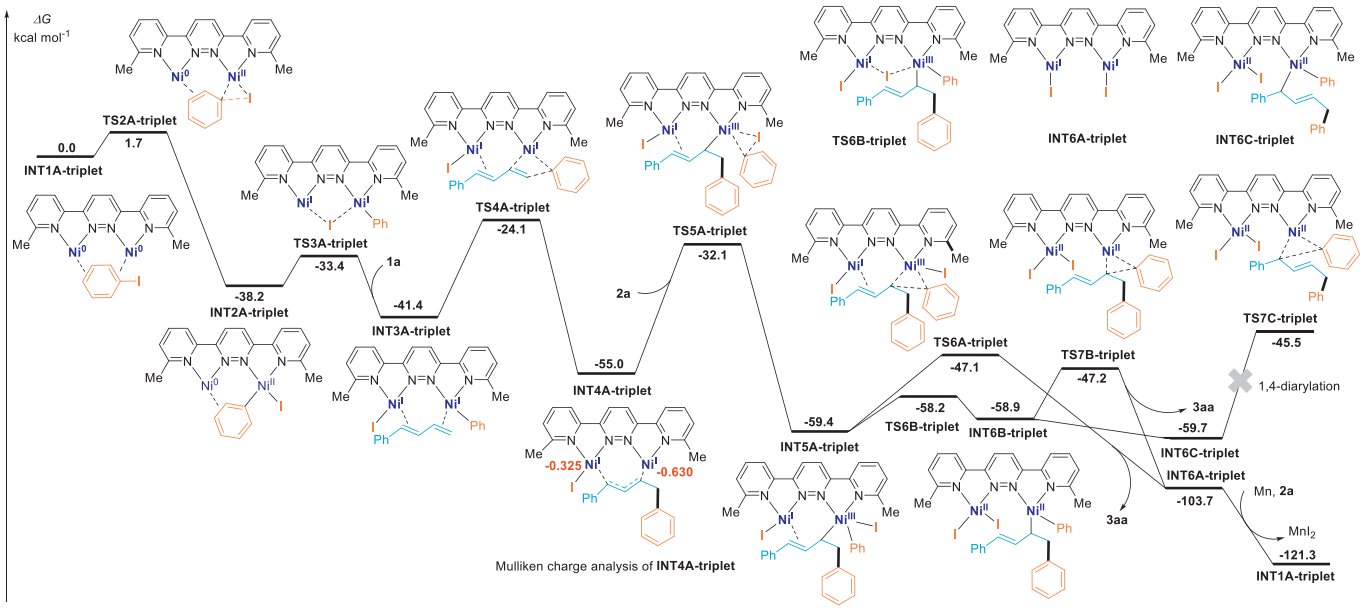
slurry mixture, which upon recrystallization in MeOH yielded a dinuclear complex **A** as characterized by X-ray crystallographic analysis (Scheme 4b). The structure is featured by a coplanar arrangement of two Ni^{II} centers with the ligand backbone. Each Ni^{II} center engages in bidentate coordination with **L7**, *via* binding with one nitrogen atom from pyridazine and another from pyridine, and the two Ni^{II} centers are bridged by an H_2O-ligand with the rest of the octahedral coordination sites being occupied by the bromide anion or water molecules. Conversely, reacting **L7** with 2.0 equiv. of NiI_2 generated a brown slurry that crystallized into a mononuclear Ni complex **B**, featuring an octahedral Ni^{II} center coordinated by four nitrogen donors from two **L7**. Both the reaction and crystallization of the two metal complexes were carried out under air conditions, and the water in the complexes originated from atmospheric moisture. Despite these well-defined structures, neither complex **A** nor **B** exhibited catalytic activity under standard conditions, leaving substrate **1a** full recovered (Scheme 4c). Intriguingly, when 2.0 equiv. of $MgCl_2$ was introduced as an additive, the reaction using complex **A** as catalyst in DMA solvent led to the formation of product **3aa** in 18 % yield. The role of additive $MgCl_2$ is likely to remove the water ligand from the complex, activate complex **A**, and lower its reduction potential, thereby facilitating the reduction of complex **A** to Ni^0 by Mn powder [113]. This outcome implies that dinuclear nickel species might serve as the active catalytic entities in this transformation. The limited efficiency of complex **A** is likely to arise from the resistance of Ni^{II} centers in methylated pyridine ligand systems to reduction into catalytically active Ni^0 states [62]. Treatment of **1a** with a stoichiometric amount of Ni^0/Mn/**L7** (2:6:1 ratio) resulted in almost no conversion of 1,3-diene. By contrast, the combination

of Ni^0/Mn/**L7** and PhI delivered a homocoupling product biphenyl in 85% GC yield (Scheme 4d). These results suggested that in the titled reaction Ni^0/**L7** would react with PhI first to initiate the reaction, and then the resulting Ni species may undergo coupling events with 1,3-diene in the diarylation process. Besides, radical clock experiment between **11**, **13**, **15** and **2a** under the current catalysis failed to obtain the ring-opening diarylation products **12**, **14** and **3aa** (Scheme 4e), indicating that the reaction might not be a single-electron transfer process. In addition, identical stereoselectivity ($E/Z > 99:1$) and yields from (*Z*)-/(*E*)-**1a** mixtures *versus* pure (*E*)-**1a** (82% yield, Scheme 4f) strongly implicate that an allyl-Ni intermediate might be formed during the catalysis. In the absence of substrate **2a**, the *E*/*Z* isomer mixture of **1a** reacted under standard conditions, and the ratio of *E*/*Z* isomers of the substrate remained unchanged after the reaction (Scheme 4g). This indicates that the alkene isomerization occurs after the migratory insertion of the Ph group into the terminal C=C double bond of the alkene. In the absence of Mn, the stoichiometric reaction of **1a**, **2a**, and Ni^0/**L7** afforded product **3aa** in 23% yield, indicating that it was a Ni^0/**L7** mediated process. The addition of Mn significantly increased the conversion of 1,3-diene, leading to the formation of **3aa** in 60% yield (Scheme 4h). These results suggested that Mn may act as a terminal reductant to reactivate the catalyst.

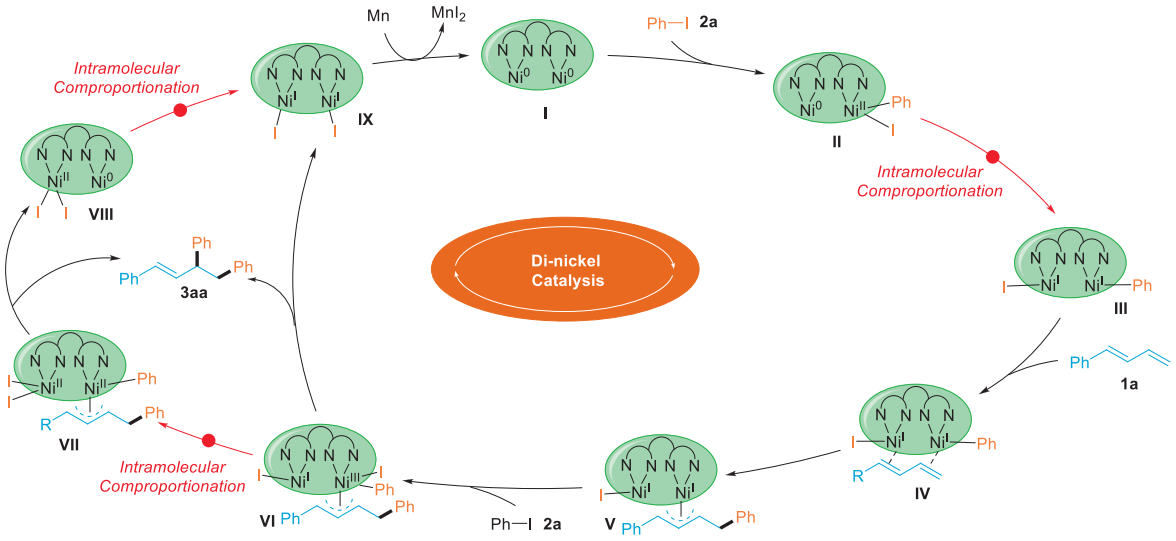
We also conducted deuterium labelling experiments to probe the potential substitution on the ligand backbone under the reaction conditions (Scheme 4i). After reacting the ligand with $Ni(COD)_2$ and quenching it with D_2O, it was found that the ligand was not deuterated. This result indicated that there was no activation of the ligand's carbon hydrogen bond during the formation of the active catalyst.

In addition to the stable Ni^{II} complexes **A** and **B**, efforts were also devoted to synthesizing dinuclear Ni^0 or Ni^I complexes supported by **L7**, as such species could provide valuable mechanistic insight (for details, see Supporting information). However, neither informative NMR or EPR signals nor crystalline products were obtained, likely due to the inherent instability of these complexes. We hypothesize that the reason for the undetectable EPR signal may be the mutual cancellation of the EPR signals from the two Ni^I centers in the dinuclear intermediate [62]. Therefore, to better understand the distinctive role played by dinuclear nickel catalysts, density functional theory (DFT) investigations was carried out at M06/6–311+*G*(d,p)-SDD/IEFPCM(THF)//PBE0-D3BJ/6–31*G*(d)-SDD level of theory. Various complexes with diverse spin multiplicities were initially calculated, and among them, the spin state of the dinuclear nickel complex characterized by a spin multiplicity of 3 emerged as the most energetically favorable, possessing the lowest energy. The intermediate **INT1A-triplet**, formed *via* the coordination of dinuclear Ni^0 with iodobenzene **2a**, was designated as the reference point for Gibbs free energy. The calculated energy profile for the catalytic cycle is presented in Scheme 5. Initially, the Ni^0 center of **INT1A-triplet** engages in an oxidative addition reaction with the C-I bond. This transformation occurs through the transition state **TS2A-triplet**, surmounting an energy barrier of 1.7 kcal/mol. The resulting intermediate, **INT2A-triplet**, then undergoes an intramolecular comproportionation step *via* the transition state **TS3A-triplet**, with an energy barrier of 4.8 kcal/mol, leading to the formation of a dinuclear Ni^I intermediate **INT3A-triplet** with the coordination of diene **1a**. Subsequently, the terminal double bond of diene **1a** undergoes migratory insertion into the Ni-Ph bond of **INT3A-triplet**, generating a η^3-allyl intermediate **INT4A-triplet**. The reversible tautomerization process of the **INT4A-triplet**, which involves the transition from η^3-allyl to η^1-allyl, effectively normalizes the initially *E*/*Z* configurations of the substrates into the most thermodynamically stable *trans*-η^3-allyl configuration (See Supporting information for details). Structural analysis of the transition state **TS4A-triplet** reveals a pronounced coordination interaction between the middle double bond of the diene and another nickel center. This coordination interaction disrupts the conjugated system of **2a**, effectively lowering the activation energy required for the terminal double bond insertion step (17.3 kcal/mol). In contrast, when the bipyridine ligand **L1** is employed, the mononuclear nickel-catalyzed migratory insertion process encounters a substantially higher energy barrier of 27.5 kcal/mol, highlighting the importance of the di-Ni diene coordination. Mulliken charge analysis provides insights into the electronic properties of **INT4A-triplet**. The nickel atom bonded to the allyl group exhibits a significantly higher electron cloud density (−0.630 e *vs.* −0.325 e), rendering it more susceptible to oxidative addition step with the second iodobenzene. Thus, the intermediate **INT4A-triplet** undergoes the second oxidative addition step with iodobenzene through the transition state **TS5A-triplet**. This step necessitates the overcoming of a free energy barrier of 22.9 kcal/mol, which represents the highest energy hurdle in the catalytic cycle and serves as the rate-determining step of the reaction. The intermediate **INT5A-triplet** undergoes a reductive elimination reaction *via* the transition state **TS6A-triplet**, with an energy barrier of 12.3 kcal/mol. This process results in the formation of the dinuclear nickel complex **INT6A-triplet** and the liberation of the diaryl-substituted product **3aa**. Alternatively, **INT5A-triplet** can generate a dinuclear Ni^{II} species **INT6B-triplet** through an intramolecular comproportionation between Ni^I and Ni^{III}. Subsequently, the reductive elimination of the Ni^{II} occurs through the transition state **TS7B-triplet**, yielding the desired product **3aa** and **INT6A-triplet**. In the presence of Mn powder as the terminal reductant, **INT6A-triplet** is reduced back to the zero-valent state, thereby completing the catalytic cycle. The intermediate **INT6B-triplet** is capable of reversibly forming the 1,4-diarylated precursor **INT6C-triplet**. Subsequently **INT6C-triplet** engages in a reductive elimination event, culminating in the generation of the 1,4-arylated by-product. This process proceeds through a transition state **TS7C-triplet** with an energy barrier of 14.2 kcal/mol. Significantly, this energy barrier exceeds that of the 1,2-diarylation process by 1.6 kcal/mol (**TS7C-triplet** *vs.* **TS6A-triplet**). Such a disparity in energy barriers serves as a pivotal determinant in ensuring the exceptional regioselectivity of the entire reaction system.

Finally, based on the mechanistic experiments and theoretical calculations, a possible reaction mechanism was proposed in Scheme 6. The dinuclear nickel intermediate **I** undergoes oxidative addition on a single Ni^0 site with iodobenzene to yield the (Ni^0, Ni^{II})-intermediate **II**, which can then undergo a rapid intramolecular single-electron transfer process accompanied by an iodide transfer to afford comproportionation product (Ni^I, Ni^I)-**III**. Intermediate **III** coordinates with the double bonds of 1,3-diene using both Ni^I centers to form intermediate **IV**, followed by the migratory insertion of the terminal carbon-carbon double bond into the Ph–Ni^I moiety, thus resulting in the formation of the Ni^I allylic intermediate **V**. The allylic-bearing Ni^I in intermediate **V,** by virtue of its enhanced nucleophilicity, can preferentialy undergo another oxidative addition with iodobenzene to generate (Ni^I, Ni^{III})-intermediate **VI**, wherein both the phenyl and allyl groups have been loaded on a single Ni^{III} site. Intermediate **VI** rapidly undergoes an intramolecular single-electron transfer to produce (Ni^{II}, Ni^{II})-intermediate **VII** [114,115], which undergoes reductive elimination to give the desired diarylated product and simultaneously generates (Ni^{II}, Ni^0)-intermediate **VIII**. Intermediate **VIII** further undergoes an intramolecular single-electron transfer to yield intermediate **IX**, which is then reduced by manganese powder to regenerate the dinuclear nickel intermeidate **I**, thus completing the catalytic cycle. An alternative pathway to yield the diarylated product is through the direct reductive elimination of intermediate **VI** to form intermediate **IX**. In the catalytic cycle, man-



Scheme 5. DFT-computed reaction pathways for the dinuclear Ni enabled reductive diarylation of dienes.



Scheme 6. The proposed mechanism.

ganese powder acts as the terminal reductant to reduce intermediate **IX** and regenerate catalyst **I**. Additionally, the catalytic cycle involves rapid intramolecular nickel comproportionation processes, which are crucial for controlling the reaction pathway. Despite the proposal of a reasonable mechanistic explanation for the complex binuclear metallic system, other reaction pathways cannot be excluded.

In summary, we have developed an efficient dinuclear nickel-catalyzed diarylation of 1,3-dienes using aryl iodides. This methodology demonstrates broad substrate compatibility across a diverse range of aryl iodides and diene substrates. Mechanistic investigations reveal that a series of redox events facilitated by intramolecular comproportionation between adjacent nickel centers within the bimetallic complex framework, which plays a pivotal role in forging the two new C–C bonds in the process. The elucidated mechanism and identified cooperative effects would provide a rational basis for future catalyst development and discovery of using related transformation modes in organometallic catalysis.

CRediT authorship contribution statement

Xiaolong Qi: Writing – original draft, Methodology. **Xueli Lv:** Writing – original draft, Methodology. **Lin Gao:** Methodology, Investigation. **Jiwen Jiao:** Methodology, Data curation. **Minyan Wang:** Writing – review & editing, Writing – original draft, Project administration. **Xiaoming Wang:** Writing – review & editing, Writing – original draft, Supervision, Project administration.

Declaration of competing interest

The authors declare that they have no known competing financial interests or personal relationships that could have appeared to influence the work reported in this paper.

Acknowledgments

The authors acknowledge financial support from the National Key R&D Program of China (No. 2022YFA1503200), the Strategic Priority Research Program of the Chinese Academy of Sciences (No. XDB1180000), the Research Funds of Hangzhou Institute for Advanced Study, UCAS (No. 2024HIAS-p003), the National Natural Science Foundation of China (Nos. 92256303, 22171278), the Shanghai Science and Technology Committee (No. 23ZR1482400), the Natural Science Foundation of Ningbo (No. 2023J034) and Open Research Fund of School of Chemistry and Chemical Engineering, Henan Normal University. We are also grateful to the High-Performance Computing Center of Nanjing University for performing the numerical calculations in this paper on its blade cluster system.

Supplementary materials

Supplementary material associated with this article can be found, in the online version, at doi:10.1016/j.cclet.2025.112189.

References

[1] N. Strater, W.N. Lipscomb, T. Klabunde, B. Krebs, Angew. Chem. Int. Ed. 35 (1996) 2024–2055.
[2] P.A. Lindahl, J. Inorg. Biochem. 106 (2012) 172–178.
[3] D.C. Powers, T. Ritter, Acc. Chem. Res. 45 (2012) 840–850.
[4] W.X. Zhang, Z.F. Xi, Org. Chem. Front. 1 (2014) 1132–1139.
[5] P. Buchwalter, J. Rosé, P. Braunstein, Chem. Rev. 115 (2015) 28–126.
[6] R.J. Eisenhart, L.J. Clouston, C.C. Lu, Acc. Chem. Res. 48 (2015) 2885–2894.
[7] N.P. Mankad, Chem. Eur. J. 22 (2016) 5822–5829.
[8] C.M. Farley, C. Uyeda, Trends Chem. 1 (2019) 497–509.
[9] J. Campos, Nat. Rev. Chem. 4 (2020) 696–702.
[10] B.D. Nath, K. Takaishi, T. Ema, Catal. Sci. Technol. 10 (2020) 12–34.
[11] W. Xu, M. Li, L. Qiao, J. Xie, Chem. Commun. 56 (2020) 8524–8536.
[12] C. Fricke, T. Sperger, M. Mendel, F. Schoenebeck, Angew. Chem. Int. Ed. 60 (2021) 3355–3366.
[13] J.A. Hueffel, T. Sperger, I. Funes-Ardoiz, et al., Science 1979 374 (2021) 1134–1140.
[14] J. Torres-Nieto, W.W. Brennessel, W.D. Jones, J.J. Garcia, J. Am. Chem. Soc. 131 (2009) 4120–4126.
[15] J. Cornella, E. Gomez-Bengoa ´, R. Martin, J. Am. Chem. Soc. 135 (2013) 1997–2009.
[16] A.H. Christian, P. Müller, S. Monfette, Organometallics 33 (2014) 2134–2137.
[17] H.X. Xu, J.B. Diccianni, J. Katigbak, et al., J. Am. Chem. Soc. 138 (2016) 4779–4786.
[18] J.B. Diccianni, C. Hu, T.N. Diao, Angew. Chem. Int. Ed. 55 (2016) 7534–7538.
[19] K. Matsubara, Y. Fukahori, T. Inatomi, et al., Organometallics 35 (2016) 3281–3287.
[20] J.B. Diccianni, C. Hu, T.N. Diao, Angew. Chem. Int. Ed. 56 (2017) 3635–3639.
[21] K. Matsubara, H. Yamamoto, S. Miyazaki, et al., Organometallics 36 (2017) 255–265.
[22] R.J. Somerville, L.V.A. Hale, E. Gomez-Bengoa ´, J. Bures ´, R. Martin, J. Am. Chem. Soc. 140 (2018) 8771–8780.
[23] R. Sun, Y.Z. Qin, S. Ruccolo, et al., J. Am. Chem. Soc. 141 (2019) 89–93.
[24] C.S. Day, R.J. Somerville, R. Martin, Nat. Catal. 4 (2021) 124–133.
[25] A.M. Borys, E.E Hevia, Chem. Commun. 60 (2024) 11052–11067.
[26] Y.Y. Zhou, C. Uyeda, Science 1979 363 (2019) 857–862.
[27] C. Uyeda, C.M. Farley, Acc. Chem. Res. 54 (2021) 3710–3719.
[28] A.B. Dürr, H.C. Fisher, I. Kalvet, K.N. Truong, F. Schoenebeck, Angew. Chem. Int. Ed. 56 (2017) 13431–13435.
[29] A. Kapat, T. Sperger, S. Guven, F. Schoenebeck, Science 1979 363 (2019) 391–396.
[30] M. Mendel, T.M. Karl, J. Hamm, et al., Nature 631 (2024) 80–86.
[31] K. Chen, H. Zhu, S. Liu, et al., J. Am. Chem. Soc. 145 (2023) 24877–24888.
[32] K. Chen, H.D. Zhu, S.X. Jiang, et al., Nat. Comm. 16 (2025) 3077.
[33] E. RIchmond, J. Moran, Synthesis 50 (2018) 499–513.
[34] M.D. Levin, S. Kim, F.D. Toste, ACS Cent. Sci. 2 (2016) 293–301.
[35] J. Twilton, C. Le, P. Zhang, et al., Nat. Rev. Chem. 1 (2017) 52.
[36] C. Zhu, H. Yue, L. Chu, M. Rueping, Chem. Sci. 11 (2020) 4051–4064.
[37] S.O. Badir, G.A. Molander, Chem 6 (2020) 1327–1339.
[38] A. Kommoju, K. Snehita, K. Sowjanya, S.B. Mukkamala, K. Padala, Chem. Commun. 60 (2024) 8946.
[39] Y. Xu, W. Zu, H. Huo, ChemCatChem 17 (2025) e202500061.
[40] J. Lu, Y. Wang, T. McCallum, N. Fu, iScience 23 (2020) 101796.
[41] C. Ma, P. Fang, D. Liu, et al., Chem. Sci. 12 (2021) 12866.
[42] C. Ma, J.F. Guo, S.S. Xu, T.S. Mei, Acc. Chem. Res. 58 (2025) 399–414.
[43] C.Y. Lin, P.P. Power, Chem. Soc. Rev. 46 (2017) 5347–5399.
[44] C.S. Day, R. Martin, Chem. Soc. Rev. 52 (2023) 6601–6616.
[45] C.S. Day, Pure Appl. Chem. 96 (2024) 437–446.
[46] R. Beck, S.A. Johnson, Organometallics 32 (2013) 2944–2951.
[47] G.Y. Yin, I. Kalvet, U. Englert, F. Schoenebeck, J. Am. Chem. Soc. 137 (2015) 4164–4172.
[48] L.M. Guard, M.M. Beromi, G.W. Brudvig, N. Hazari, D.J. Vinyard, Angew. Chem. Int. Ed. 54 (2015) 13352–13356.
[49] I. Kalvet, Q.Q. Guo, G.J. Tizzard, F. Schoenebeck, ACS Catal. 7 (2017) 2126–2132.
[50] D. Balcells, A. Nova, ACS Catal. 8 (2018) 3499–3515.
[51] M.M. Beromi, G.W. Brudvig, N. Hazari, H.M.C. Lant, B.Q. Mercado, Angew. Chem. Int. Ed. 58 (2019) 6094–6098.
[52] N.A. Till, S. Oh, D.W.C. MacMillan, M.J. Bird, J. Am. Chem. Soc. 143 (2021) 9332–9337.
[53] A. Bismuto, P. Finkelstein, P. Müller, B. Morandi, Helv. Chim. Acta 104 (2021) e2100177.
[54] C.S. Day, A. Rentería-Gómez, S.J. Ton, et al., Nat. Catal. 6 (2023) 244–253.
[55] S.H. Newman-Stonebraker, T.J. Raab, H. Roshandel, A.G. Doyle, J. Am. Chem. Soc. 145 (2023) 19368–19377.
[56] D.C. Powers, B.L. Anderson, D.G. Nocera, J. Am. Chem. Soc. 135 (2013) 18876–18883.
[57] S.Z. Tasker, E.A. Standley, T.F. Jamison, Nature 509 (2014) 299–309.
[58] E.C. Hansen, D.J. Pedro, A.C. Wotal, et al., Nat. Chem. 8 (2016) 1126–1130.
[59] R.J. Somerville, C. Odena, M.F. Obst, et al., J. Am. Chem. Soc. 142 (2020) 10936–10941.
[60] A.L. Aguirre, N.L. Loud, K.A. Johnson, D.J. Weix, Y. Wang, Chem. Eur. J. 27 (2021) 12981–12986.
[61] S.I. Ting, W.L. Williams, A.G. Doyle, J. Am. Chem. Soc. 144 (2022) 5575–5582.
[62] H.T. Huang, J.L. Alvarez-Hernandez, N. Hazari, B.Q. Mercado, M.R. Uehling, ACS Catal. 14 (2024) 6897–6914.
[63] M.E. Akana, S. Tcyrulnikov, B.D. Akana-Schneider, et al., J. Am. Chem. Soc. 146 (2024) 3043–3051.
[64] W.A. Butte, F.H. Case, Notes 26 (1961) 4690–4692.
[65] A. Tiripicchio, A.M.M. Lanfredi, M. Ghedini, F. Neve, Chem. Commun. (1983) 1134.
[66] A.M.M. Lanfredi, A. Tiripicchio, F. Ugozzoli, Dalton Trans. 1988 (1988) 651–656.
[67] N. Tsukada, T. Sato, H. Mori, et al., J. Org. Chem. 627 (2001) 121–126.
[68] R. Dorta, L. Konstantinovski, L.J.W. Shimon, Y. Ben-David, D. Milstein, Eur. J. Inorg. Chem. (2003) 70–76.
[69] M. Zhou, K.R. Jain, A. Günyar, et al., Eur. J. Inorg. Chem. 2009 (2009) 2907–2914.
[70] M.R. McDevitt, F.L. Urbach, Polyhedron 67 (2014) 405–409.
[71] N. Marino, R. Bruno, A. Bentama, et al., CrystEngComm 21 (2019) 917.
[72] C.E.I. Knappke, S. Grupe, D. Grtner, et al., Chem. Eur. J. 20 (2014) 6828–6842.
[73] T. Moragas, A. Correa, R. Martin, Chem. Eur. J. 20 (2014) 8242–8258.
[74] D.A. Everson, D.J. Weix, J. Org. Chem. 79 (2014) 4793–4798.
[75] D.J. Weix, Acc. Chem. Res. 48 (2015) 1767–1775.
[76] J. Gu, X. Wang, W.C. Xue, H.G. Gong, Org. Chem. Front. 2 (2015) 1411–1421.
[77] X. Wang, Y.J. Dai, H.G. Gong, Top. Curr. Chem. 374 (2016) 43.
[78] E.L. Lucas, E.R. Jarvo, Nature Rev. Chem. 1 (2017) 1–7.
[79] M.E. Greaves, E.L.B.J. Humphreya, D.J. Nelson, Catal. Sci. Technol. 11 (2021) 2980–2996.
[80] S.S. Geng, C.Q. Shi, B.H. Guo, et al., ACS Catal. 13 (2023) 15469–15480.
[81] Z.Z. Zhao, P. Guo, X.B. Pang, X.Z. Shu, Acc. Chem. Res. 57 (2024) 3356–3374.
[82] Y.X. Gong, J. Hu, C.B. Qiu, H.G. Gong, Acc. Chem. Res. 57 (2024) 1149–1162.
[83] J. Derosa, O. Apolinar, T. Kang, V.T. Tran, K.M. Engle, Chem. Sci. 11 (2020) 4287.
[84] Y.C. Luo, C. Xu, X.G. Zhang, Chin. J. Chem. 38 (2020) 1371–1394.
[85] H.Y. Tu, S.Q. Zhu, F.L. Qing, L.L. Chu, Synthesis 52 (2020) 1346–1356.
[86] L.M. Wickham, R. Giri, Acc. Chem. Res. 54 (2021) 3415–3437.
[87] Y. Wei, L.Q.H. Lin, B.C. Lee, M. Koh, J. Acc. Chem. Res. 56 (2023) 3292–3312.
[88] Y.C. Liu, F.Y. Li, M.U.S. Bhat, L. Tian, et al., Chin. J. Chem. 43 (2025) 3637–3658.
[89] Z. Li, L. Liu, Chin. J. Catal. 36 (2015) 3–14.
[90] Q. Lin, T.N. Diao, J. Am. Chem. Soc. 141 (2019) 17937–17948.
[91] J.B. Diccianni, T.N. Diao, Trends Chem. 45 (2019) 1–15.
[92] J. Diccianni, Q. Lin, T.N. Diao, Acc. Chem. Res. 53 (2020) 906–919.
[93] T. Yanagi, R.J. Somerville, K. Nogi, R. Martin, H. Yorimitsu, ACS Catal. 10 (2020) 2117–2123.
[94] L.E. Ehehalt, O.M. Beleh, I.C. Priest, et al., Chem. Rev. 124 (2024) 13397–13569.
[95] T.J. Anderson, G.D. Jones, D.A. Vicic, J. Am. Chem. Soc. 126 (2004) 8100–8101.
[96] G.D. Jones, C. McFarland, T.J. Anderson, D.A. Vicic, Chem. Commun. (2005) 4211–4213.
[97] G.D. Jones, J.L. Martin, C. McFarland, et al., J. Am. Chem. Soc. 128 (2006) 13175–13183.
[98] K. Zhang, M. Conda-Sheridan, S.R. Cooke, J. Louie, Organometallics 30 (2011) 2546–2552.
[99] Z. Li, Y.Y. Jiang, Y. Fu, Chem. Eur. J. 18 (2012) 4345–4357.
[100] J. Breitenfeld, M.D. Wodrich, X. Hu, Organometallics 33 (2014) 5708–5715.
[101] M.M. Beromi, A. Nova, D. Balcells, et al., J. Am. Chem. Soc. 139 (2017) 922–936.
[102] M.M. Beromi, G. Banerjee, G.W. Brudvig, N. Hazari, B.Q. Mercado, ACS Catal. 8 (2018) 2526–2533.
[103] D. Anthony, Q. Lin, J. Baudet, T.N. Diao, Angew. Chem. Int. Ed. 58 (2019) 3198.
[104] D. Anthony, T.N. Diao, Synlett 31 (2020) 1443–1447.
[105] W. Zhang, D. Ji, Y. Li, et al., ACS Catal. 12 (2022) 2158–2165.
[106] W. Chen, L. Yu, Y. Pan, S. Ni, Y. Wang, Org. Lett. 25 (2023) 9225–9230.
[107] W.S. Zhang, D.W. Ji, Y. Li, et al., Nat. Comm. 14 (2023) 651.
[108] B. Lu, X. Liang, J. Zhang, et al., J. Am. Chem. Soc. 143 (2021) 11799–11810.

[109] K. Chen, H. Zhu, Y. Li, et al., ACS Catal. 11 (2021) 13696–13705.
[110] Y. Yang, B. Lu, G. Xu, X.M. Wang, ACS Cent. Sci. 8 (2022) 581–589.
[111] Q.L. Cai, H. Rao, S.J. Li, et al., Chem 10 (2024) 265–282.
[112] Y. Lan, P. Liu, Z. Fang, et al., Org. Chem. Front. 11 (2024) 6319–6326.
[113] Y. Ye, H. Chen, J.L. Sessler, H. Gong, J. Am. Chem. Soc. 141 (2019) 820–824.
[114] D.A. Cagan, D. Bím, N.P. Kazmierczak, R.G. Hadt, ACS Catal. 14 (2024) 9055–9076.
[115] J.W. Sun, Á. Péter, J.Y. He, et al., Science 387 (2025) 1377–1383.